9-21-2010

Discovery of cyclic spot activity on the G8 giant HD 208472

Orkun Özdarcan
Ege University

Serdar Evren
Ege University

Klaus G. Strassmeier
Astrophysical Institute Potsdam

Thomas Granzer
Astrophysical Institute Potsdam

Gregory W. Henry
Tennessee State University

Recommended Citation

Özdarcan, O., Evren, S., Strassmeier, K., Granzer, T. and Henry, G. (2010), Discovery of cyclic spot activity on the G8 giant HD 208472. Astron. Nachr., 331: 794-806. https://doi.org/10.1002/asna.201011413

Astron. Nachr. / AN **331**, No. 8, 794 – 806 (2010) / **DOI** 10.1002/asna.201011413

Discovery of cyclic spot activity on the G8 giant HD 208472⋆

O. Özdarcan[1,2,⋆⋆], **S. Evren**[1], **K.G. Strassmeier**[2], **T. Granzer**[2], and **G.W. Henry**[3]

[1] Ege University, Faculty of Sciences, Astronomy and Space Sciences Dept., 35100 Bornova - Izmir, Turkey
[2] Astrophysical Institute Potsdam (AIP), An der Sternwarte 16, D-14482 Potsdam, Germany
[3] Center of Excellence in Information Systems, Tennessee State University (TSU), 3500 John A. Merritt Blvd., Box 9501, Nashville, TN 37209, USA

Received 2010 Jul 5, accepted 2010 Aug 10
Published online 2010 Oct 1

Key words binaries: close – stars: activity – stars: individual (HD 208472) – starspots – techniques: photometric

We present and analyze 17 consecutive years of $UBVRI$ time-series photometry of the spotted giant component of the RS CVn binary HD 208472. Our aim is to determine the morphology and the evolution of its starspots by using period-search techniques and two-spot light-curve modelling. Spots on HD208472 always occur on hemispheres facing the observer during orbital quadrature and flip their location to the opposite hemisphere every approximately six years. The times when the spots change their preferential hemisphere correspond to times when the light curve amplitudes are the smallest and when abrupt changes of the photometric periods are observed. During these times the star is also close to a relative maximum brightness, suggesting a vanishing overall spottedness at each end of the previous cycle and the start of a new one. We find evidence for a 6.28±0.06-yr brightness cycle, which we interpret to be a stellar analog of the solar 11-year sunspot cycle. We also present clear evidence for a brightening trend, approximated with a 21.5±0.5-yr period, possibly due to a stellar analog of the solar Gleissberg cycle. From the two-spot modelling we also determine an upper limit for the differential-rotation coefficient of $\alpha = \Delta P/P$ of 0.004±0.010, which would be fifty times weaker than on the Sun.

1 Introduction

Attention was drawn to HD 208472 (V2075 Cyg) only after its strong Ca II H and K emission was discovered by W. Bidelman in 1991. Henry et al. (1995) discovered its photometric variability, determined a photometric period of 22.54 days, and presented a preliminary orbital period of 22.6 days, showing this star to be a synchronous rotator. They concluded that the system is very active as evidenced by its large-amplitude V-band variations of $0\overset{\mathrm{m}}{.}36$ in 1993 and Hα-line emission well above the continuum. Later, Fekel et al. (1999) presented the orbital elements, refined the orbital period to 22.62293 days and confirmed the G8III classification from Henry et al. (1995). A more comprehensive photometric study by Strassmeier et al. (1999) witnessed a continuous decrease of its light-curve amplitude from $0\overset{\mathrm{m}}{.}12$ in late 1996 to $0\overset{\mathrm{m}}{.}07$ in mid 1997. Such large changes are typical only for the most active stars. The photometric period was confirmed to be 22.42±0.12 days. The star was also detected as a variable star in the Hipparcos epoch photometry with a period of 22.32 days (Koen & Eyer 2002). Just recently, Erdem et al. (2009) presented new multi-band CCD photometry acquired in 2006 and 2007.

Weber et al. (2001) presented the first (and so far only) Doppler images of HD 208472, based on observations taken at the U.S. National Solar Observatory between 1996 and 1997. These images were refined and discussed in more detail in Weber (2004) and Weber et al. (2005). All maps showed pronounced spot activity located at low to intermediate latitudes. No polar spot, as seen on many other rapidly-rotating giants, was observed. While a sheared-image, line-profile inversion suggested anti-solar differential rotation with a differential-rotation coefficient of $\alpha = -0.04 \pm 0.02$, a direct cross-correlation analysis of the three available Doppler images revealed uncertainties larger than the above value. Therefore, Weber (2004) and Weber et al. (2005) did not claim to have resolved differential rotation of HD 208472. For comparison, a summary of existing Doppler images is given in Strassmeier (2009).

In this paper we present and analyze 17 consecutive years of time-series photometry of HD 208472. The sampling is such that we can easily see the rotational modulation within every one of the 17 observing seasons. Such unique data sets are possible with the advent of automatic photometric telescopes (APTs) and their continuous operation, e.g., at Fairborn Observatory (Genet et al. 1986; Henry 1995a; Granzer et al. 2001). We present and briefly describe the various telescopes and instrumental set ups in Sect. 2. In Sect. 3, we consider the global, long-term behavior of the spots on HD 208472, and in Sect. 4, we analyze the rotational modulation in the 17 annual light curves. We present a summary and our conclusions in Sect. 5.

⋆ Based on data obtained with the Amadeus T7 Automatic Photoelectric Telescope at Fairborn Observatory, jointly operated by the University of Vienna and AIP, the Tennessee State University T3 0.4 m APT at Fairborn Observatory, operated by Tennessee State University, and the telescopes of the Ege University Observatory in Izmir.

⋆⋆ Corresponding author: orkun.ozdarcan@ege.edu.tr

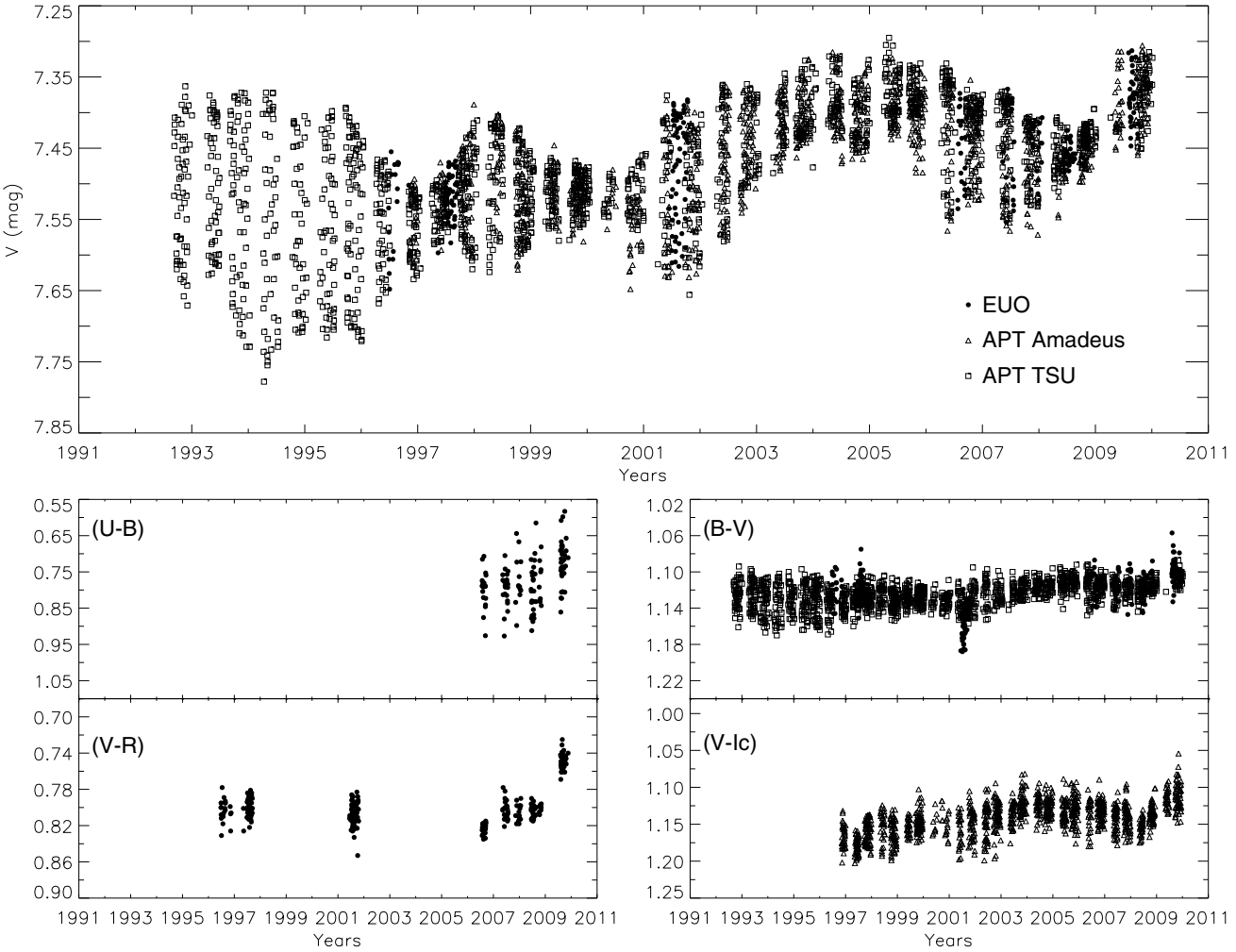

Fig. 1 Seventeen years of V-band photometry of HD 208472 (*upper panel*) together with all available color indices (*lower panels*). Open squares denote data from the TSU 0.40 m APT, open triangles denote data from the 0.75 m Amadeus APT, and filled circles represent EUO data.

2 Observations and data reductions

Photometry was collected from three sources as summarized in Table 1. Firstly, the TSU 0.40 m APT, located at Fairborn Observatory in southern Arizona, produced a continuous 17-year set of Johnson B and V measurements since 1992. For details on the data reduction procedures and performance of this telescope see Henry (1995b). Secondly, a total of 13 years of continuous Johnson-Cousin $VI_{\rm C}$ data, beginning in 1996, were acquired with the 0.75 m Vienna University/AIP APT "Amadeus", also located at Fairborn Observatory. The Vienna/AIP APT is optimized for the red part of the spectrum with an EMI-9828 phototube and Johnson-Cousins filters. For more details see Strassmeier et al. (1997). Thirdly, numerous Johnson $UBVR$ and Strömgren $uvby\beta$ observations were made between 1996 and 2010 with the 0.48 m Cassegrain (A48) and the 0.30 m Schmidt-Cassegrain (T30) telescopes at Ege University Observatory (EUO). An Optec SSP-5 photometer was used on both EUO telescopes.

Nightly means of the EUO observations were created from 6–8 individual readings and were corrected for atmospheric extinction as described in Hardie (1962). Its precision of a nightly mean was usually below $0\overset{\rm m}{.}01$ in V. Transformation of the EUO observations to the standard Johnson and Strömgren systems was performed with coefficients determined from the 2009 observations with the SSP-5 photometer on telescope T30. Nine stars from the list of Andruk et al. (1995) were observed for the Johnson passbands; 15 stars from the catalogue of Hauck & Mermilliod (1995) were used for the Strömgren passbands. We list the transformation coefficients in the appendix.

HD 208916 was used as comparison star for both the TSU and the EUO data. The Vienna/AIP APT used HD 208431 as its comparison star but the TSU/EUO comp star, HD 208916, as the check star. Therefore, we employed the variable-minus-check star differential magnitudes from the Amadeus APT to place all the observations on the same brightness scale.

Table 1 Summary of photometric observations. $\sigma_{\rm ext}(V)$ denotes the average external precision of the data set in millimagnitudes in the V bandpass. N is the total number of data points. Δt is the time coverage.

Telescope	Filters	Δt	N	$\sigma_{\rm ext}$
0.40 m TSU APT	BV	1992.5–2009.99	1691	4
0.75 m Amadeus APT	$VI_{\rm C}$	1996.8–2010.1	1418	3.2
0.48 m EUO A48	BVR	1996.5–1997.7	66	6
0.30 m EUO T30	BVR	2001.5–2001.7	64	6
0.30 m EUO T30	$UBVR$	2006.5–2009.9	132	8
0.30 m EUO T30	$uvby\beta$	2009.59–2009.81	36	7

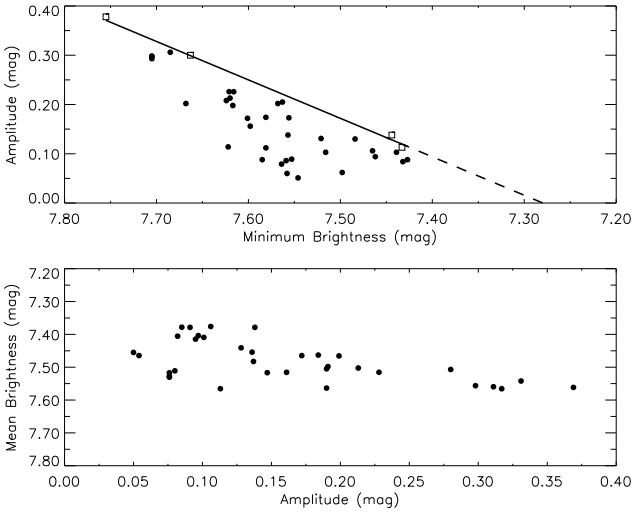

Fig. 2 Amplitude-brightness relations in Johnson V. The top panel shows the peak-to-peak amplitudes plotted with respect to the respective brightness minimum. The line is a linear fit to the data of the upper envelope. Its zero point indicates the unspotted magnitude where the amplitude becomes zero ($V \approx 7\overset{\rm m}{.}28$). The bottom panel plots the mean V brightness versus the peak-to-peak amplitude. It indicates a weak trend that larger amplitudes occur when the star is fainter.

3 Global photometric analysis

3.1 Brightness and color variations

Figure 1 shows all 17 years of V-band photometry of HD 208472 together with all available color indices. A long-term trend in the sense of a continuous increase of the overall brightness by $\approx 0\overset{\rm m}{.}1$ with time is evident. Also note that the light-curve minima increased more dramatically than the light-curve maxima. Usually, the maximum light levels remained fairly stable except during times when considerable amplitude changes were observed. For the first half of the whole data (from 1992 to 2001), the mean brightness seems relatively constant when compared to the individual light-curve amplitudes. During the second half (from 2001 to 2009), the light-curve amplitudes seem relatively constant while the mean brightness dramatically changed. In any case, the assumption of a constant amplitude and averaged brightness would cause slightly erroneous astrophysical parameters if derived solely from photometric data (see Sect. 3.3 and Fig. 4).

All color indices get systematically bluer towards the end of our data in early 2010. Not too much can be said about $(U-B)$ and $(V-R)$ due to the relative sparsity of data but the trend is even evident in these indices. On the other hand, when $(B-V)$ and $(V-I_{\rm C})$ are compared, it is seen that the red color shows on average more pronounced variations than the blue color, which indicates that the variations are dominantly due to less and less cool spots, rather than more warm plages or faculae.

3.2 Mean brightness, amplitudes and the unspotted brightness

To investigate the seasonal changes of the mean brightness, the light-curve amplitudes and the photometric period, we divided the V data into 35 subsets. We obtain the average of the maximum and minimum magnitudes separately in each subset and then calculate the average of the mean maximum and the mean minimum magnitudes and denote it the mean brightness for corresponding data set. To calculate light curve amplitudes of the sets, we consider the differences between mean maximum and mean minimum magnitudes in each set. In Fig. 2, we show the mean brightness versus the light curve amplitude (upper panel) and the light curve amplitude versus the minimum light level (lower panel). The decrease of the mean brightness with increased amplitude indicates again the preference of cool spots over warm, faculae-like structures on the stellar surface. This becomes even more evident when individual light curves are investigated both in brightness and color (see later Sect. 4). Color indices get redder at times that correspond to light minima.

The minimum brightness versus amplitude plot in Fig. 2 shows that the star appears generally brighter when the amplitude is smaller. By using the method given by Oláh et al. (1997), we can estimate the unspotted brightness, i.e. the brightness when the amplitude is zero. For that purpose, we consider the points that define the upper envelope (open squares in Fig. 2) and apply a linear fit to them. The fit intersects the minimum-brightness axis at about $7\overset{\rm m}{.}28$, where the amplitude would be zero, i.e., the star is unspotted. That value almost coincides with the observed maximum light level during the year 2009/10. Therefore, we may state that the star was at, or very close to, its unspotted brightness in at least that observing season. The long-term V-amplitude decrease also suggests a decrease of the spotted area, while the additional blueing of the average color variations suggest an increase of the spot temperature towards 2010. Combining

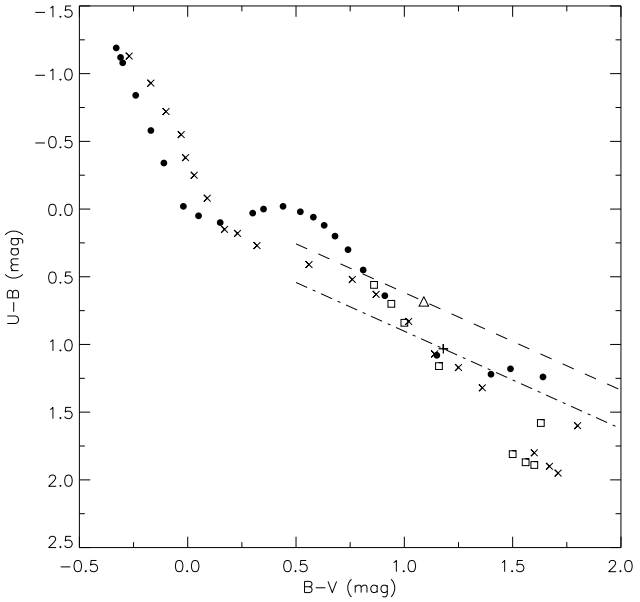

Fig. 3 HD 208472 in the UBV color-color diagram. The open triangle ($\triangle$) represents the observed color values from Table 2. The dashed line is its reddening line with a slope of 0.72. The plus sign ($+$) shows the place of the star after the $U-B$ and $B-V$ excesses were removed. The dashed-dotted line shows its reddening. Standard-star data were taken from Drilling & Landolt (2000) and are shown as filled circles for main sequence stars, crosses for supergiants and open squares for class-III giants.

these changes with the overall brightness variation, we conclude that the activity level of the star considerably changes with time. We will model this behavior more quantitatively in Sect. 4.

3.3 Interstellar reddening and astrophysical parameters

As HD 208472 is a class III giant, it is important to determine the $E(B-V)$ color excess accurately in order to find the intrinsic photometric indices and therefore the star's effective temperature. Unfortunately, the galactic coordinates of the star, $\ell = 92\overset{\circ}{.}8408$, $b = -7\overset{\circ}{.}9172$, do not permit to use any particular extinction law because the extinction can not be determined reliably for this galactic latitude range of $-10^\circ < b < 10^\circ$. At this point, we rely on our standard Johnson $UBVRI$ measurements during the year 2009, when the star was close to its unspotted brightness, as determined above. We then calculate the unspotted brightness and the colors, both for Johnson and Strömgren data, from the maximum brightness level in 2009 and list them in Table 2.

Figure 3 shows the star in the UBV color-color diagram by assuming $E(U-B)/E(B-V)$=0.72 (open triangle) and with respect to the standard-star data from Drilling & Landolt (2000). The resulting reddening would be $E(B-V)$ = $0\overset{\mathrm{m}}{.}248$ and the corresponding $(B-V)_0$ is $0\overset{\mathrm{m}}{.}842$. Such a blue $B-V$ would indicates a G4–5 spectral type rather than the G8(III) classification obtained by Henry et al. (1995), the latter based of high-resolution spectroscopy. In fact, we

Table 2 Unspotted brightness and colors of HD 208472 (from 2009 observations).

Johnson	Strömgren
$V = 7\overset{\mathrm{m}}{.}323 \pm 0\overset{\mathrm{m}}{.}007$	$y = 7\overset{\mathrm{m}}{.}267 \pm 0\overset{\mathrm{m}}{.}010$
$U-B = 0\overset{\mathrm{m}}{.}682 \pm 0\overset{\mathrm{m}}{.}068$	$b-y = 0\overset{\mathrm{m}}{.}650 \pm 0\overset{\mathrm{m}}{.}013$
$B-V = 1\overset{\mathrm{m}}{.}090 \pm 0\overset{\mathrm{m}}{.}012$	$m_1 = 0\overset{\mathrm{m}}{.}170 \pm 0\overset{\mathrm{m}}{.}028$
$V-R = 0\overset{\mathrm{m}}{.}739 \pm 0\overset{\mathrm{m}}{.}010$	$c_1 = 0\overset{\mathrm{m}}{.}420 \pm 0\overset{\mathrm{m}}{.}074$
$V-I_C = 1\overset{\mathrm{m}}{.}106 \pm 0\overset{\mathrm{m}}{.}020$	$H_\beta = 2\overset{\mathrm{m}}{.}650 \pm 0\overset{\mathrm{m}}{.}034$

Table 3 Dereddened, unspotted brightness and colors of HD 208472.

Johnson	Strömgren
$V_0 = 6\overset{\mathrm{m}}{.}929$	$y_0 = 6\overset{\mathrm{m}}{.}873$
$(U-B)_0 = 0\overset{\mathrm{m}}{.}940$	$(b-y)_0 = 0\overset{\mathrm{m}}{.}560$
$(B-V)_0 = 1\overset{\mathrm{m}}{.}053$	$(m_1)_0 = 0\overset{\mathrm{m}}{.}140$
$(V-R)_0 = 0\overset{\mathrm{m}}{.}640$	$(c_1)_0 = 0\overset{\mathrm{m}}{.}400$

believe that HD 208472 exhibits a $U-B$ and $B-V$ excess that could be the result of bright chromospheric structures like faculae. Amado (2003) investigated the effects of chromospheric activity on the mean colors of active late-type stars and suggested a mean excess value $0\overset{\mathrm{m}}{.}35$ in $U-B$ and $0\overset{\mathrm{m}}{.}09$ in $B-V$ for luminosity class III giants. By removing this mean excess from the $U-B$ and $B-V$ colors of HD 208472 (the revised $U-B$ and $B-V$ values are then $1\overset{\mathrm{m}}{.}032$ and $1\overset{\mathrm{m}}{.}180$, respectively) the resulting $E(B-V)$ is $0\overset{\mathrm{m}}{.}127$, instead of $0\overset{\mathrm{m}}{.}248$, and leads to $(B-V)_0 = 1\overset{\mathrm{m}}{.}053$. This color indicates a G8-K0 spectral type, in better agreement with the result of Henry et al. (1995). With $E(B-V)$ = $0\overset{\mathrm{m}}{.}127$, we also calculate the unreddened Strömgren brightness and colors using the relations in Fitzpatrick (1999) and references therein (see his Table 2). Our final de-reddened brightness and colors of HD 208472 are summarized in Table 3.

The effective temperature of the star is estimated from $(B-V)_0$ to be 4540 K according to the calibration by Drilling & Landolt (2000), 4750 K according to the calibration by Flower (1996), and 4790 K according to Gray (2005). In this paper, we adopt the calibration by Flower (1996) and use 4750 K for our further analysis. Its typical error is 100 K for a star of this color. Metallicity can be determined from the Strömgren $(b-y)_0$ and $(m_1)_0$ indices. With the aid of the relations given, e.g., by Hilker (2000), we find [Fe/H] = –0.50±0.25. Due to its large error, we just interpret this metallicity to be subsolar. There is a clear need for a spectroscopic analysis to either confirm or to refine this [Fe/H] value.

By combining our photometry with the refined Hipparcos parallax of 6.55 ± 0.53 mas (van Leeuwen 2007), we calculate distance and absolute brightness and list them in Table 4. For the inclination, we adopt the $v \sin i$ value of 19.7 ± 1 km s^{-1} from Fekel et al. (1999), assume the orbital period to be equal to the rotation period, and a radius from

Table 4 Absolute photometric parameters of HD 208472. The bolometric correction, B.C., was taken from Flower (1996).

Parameter	Value
V_0	$6\overset{\mathrm{m}}{.}929$
$E(B-V)$	$0\overset{\mathrm{m}}{.}127$
A_V	$0\overset{\mathrm{m}}{.}394$
R (assumed)	3.1
$(B-V)_0$	$1\overset{\mathrm{m}}{.}053 \pm 0\overset{\mathrm{m}}{.}012$
$(b-y)_0$	$0\overset{\mathrm{m}}{.}560 \pm 0\overset{\mathrm{m}}{.}013$
$T_{\rm eff}$ (K)	4750 ± 100
B.C.	–0.437
Hipparcos distance (pc)	153^{+13}_{-11}
M_V	$1\overset{\mathrm{m}}{.}011 \pm 0\overset{\mathrm{m}}{.}25$
$M_{\rm bol}$	$0\overset{\mathrm{m}}{.}574$
$v \sin i$ (km s^{-1})	19.7 ± 1.0
Inclination ($^\circ$)	60 ± 8
Radius ($R_\odot$)	10.09 ± 0.56
Luminosity ($L_\odot$)	46 ± 3
[Fe/H]	-0.50 ± 0.25

the Stefan-Boltzmann law by using a solar $M_{\rm bol}$ value of $4\overset{\mathrm{m}}{.}74$, and obtain 60°. Note that the uncertainty of the inclination of just 8° is mainly from the uncertainty of the $v \sin i$ measure, the actual error is likely larger.

3.4 A spot cycle from mean brightness variations

Undulating variations in overall brightness of the star beyond the simple rotational modulation may indicate the existence of a spot cycle analogous to the solar 11-year cycle. Although the first half of the whole light curve (from 1992 to 2001) shows almost none or at least very small variations of the mean brightness, but rather large variation in individual light curve amplitudes, assuming a truly constant mean brightness might oversimplify the situation because we observe a clear long-term trend in mean brightness. We applied a standard Fourier transform (FT) analysis to the V data by using the Period04 program (Lenz & Breger 2005). The brightening trend in Fig. 1 can be represented by a harmonic with a period of 21.5±0.5 years, significantly longer than the 17 years of time coverage of the data. Nevertheless, it might at least be an indication of a cycle like the Gleissberg cycle for the Sun (e.g. Kolláth & Oláh 2009). We then prewhiten the data with that period and treat the residuals again by means of a Fourier fit and find a period of 6.28±0.06 years. This period seems reasonably well established with respect to the time coverage of the data and thus suggests a true spot cycle. Figure 4 shows the mean brightness variation and the residuals after pre-whitening with a 21.5-yr period (lower panel) together with the fit by a 6.28-yr harmonic.

3.5 Photometric period variations

Straightforward solar-stellar analogy explains variations in the photometric period as being due to latitudinal migration of spots on a differentially rotating surface (Hall 1972; Strassmeier & Bopp 1992). The migration could be induced gradually due to, e.g., meridional circulation or could be abruptly when a current spot's lifetime ends and another spot at a different latitude appears. However, complex evolutionary morphology changes may also contribute to (photometric) period variations. Due to the shearing force of a differentially rotating surface, the resulting break up of large spots or spot clusters that spread over a certain latitude range may also give rise to photometric period variations (Strassmeier et al. 1994; Fekel et al. 2002; see also the starspot reviews by Berdyugina 2005 and Strassmeier 2009).

Table 5 Photometric periods (with errors) in days, the light curve V amplitudes in magnitudes, and the residual V brightness with respect to the 21.5-years approximation as shown in the top panel of Fig. 4. Out of the 35 data subsets, just data set #16 did not allow to determine a unique period due to its sparse data coverage.

Set	Year	Period (day)	Amplitude (mag)	Residuals (mag)
1	1992.82	22.573 ± 0.091	0.273	–0.003
2	1993.40	22.437 ± 0.091	0.213	–0.016
3	1993.84	22.482 ± 0.046	0.329	0.017
4	1994.39	22.573 ± 0.092	0.382	0.030
5	1994.90	22.528 ± 0.091	0.294	0.020
6	1995.42	22.528 ± 0.046	0.309	0.026
7	1995.87	22.573 ± 0.092	0.302	0.018
8	1996.42	22.528 ± 0.091	0.183	0.022
9	1996.93	22.124 ± 0.176	0.118	0.025
10	1997.47	21.524 ± 0.209	0.079	–0.010
11	1997.86	22.899 ± 0.142	0.170	–0.019
12	1998.39	22.391 ± 0.135	0.192	–0.031
13	1998.87	22.573 ± 0.092	0.155	–0.006
14	1999.40	22.124 ± 0.220	0.086	–0.004
15	1999.86	22.124 ± 0.220	0.077	0.010
16	2000.40	...	...	...
17	2000.86	22.619 ± 0.184	0.081	0.043
18	2001.48	22.391 ± 0.090	0.220	0.040
19	2001.86	22.036 ± 0.131	0.216	0.037
20	2002.42	22.758 ± 0.093	0.213	0.009
21	2002.86	22.302 ± 0.134	0.126	–0.007
22	2003.45	21.734 ± 0.340	0.089	–0.022
23	2003.83	22.302 ± 0.179	0.089	–0.025
24	2004.42	22.758 ± 0.280	0.100	–0.043
25	2004.83	22.528 ± 0.183	0.097	–0.007
26	2005.42	22.482 ± 0.182	0.086	–0.031
27	2005.83	22.604 ± 0.245	0.100	–0.003
28	2006.39	22.666 ± 0.139	0.199	0.059
29	2006.82	22.391 ± 0.090	0.127	0.051
30	2007.42	22.391 ± 0.090	0.165	0.061
31	2007.88	22.437 ± 0.091	0.120	0.077
32	2008.42	22.852 ± 0.282	0.063	0.056
33	2008.83	22.212 ± 0.844	0.055	0.042
34	2009.40	22.346 ± 0.180	0.106	–0.043
35	2009.80	22.302 ± 0.090	0.138	–0.046

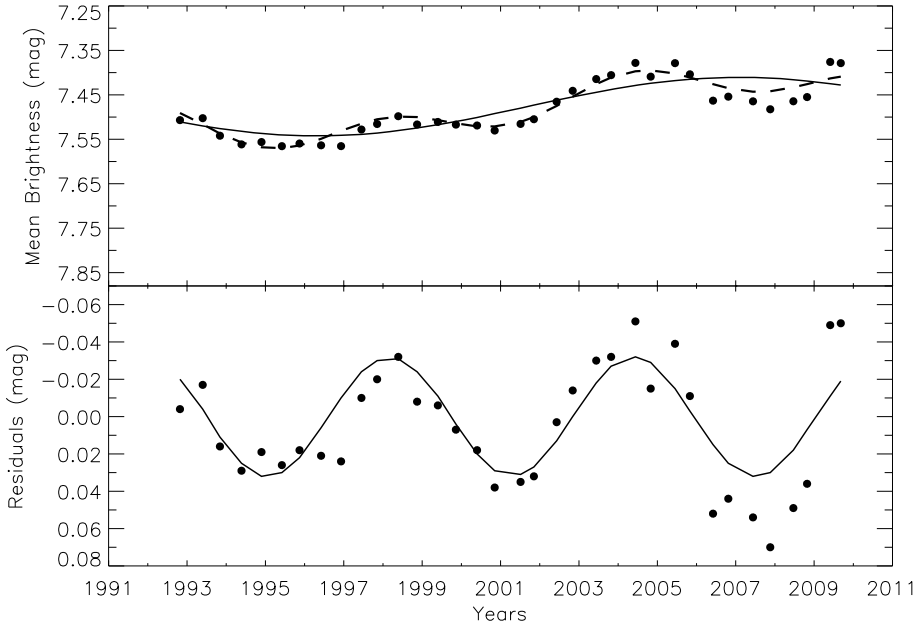

Fig. 4 Mean brightness variations (dots, *upper panel*) and their residuals (dots, *lower panel*). The lines are harmonic fits. In the upper panel, the continuous line represents a 21.5-yr period (rather a trend due to the limited time span of the data), while the dashed line represents a superposition of this and a 6.28-yr period. In the lower panel, we removed the trend and plot the data again together with the 6.28-yr period as a solid line.

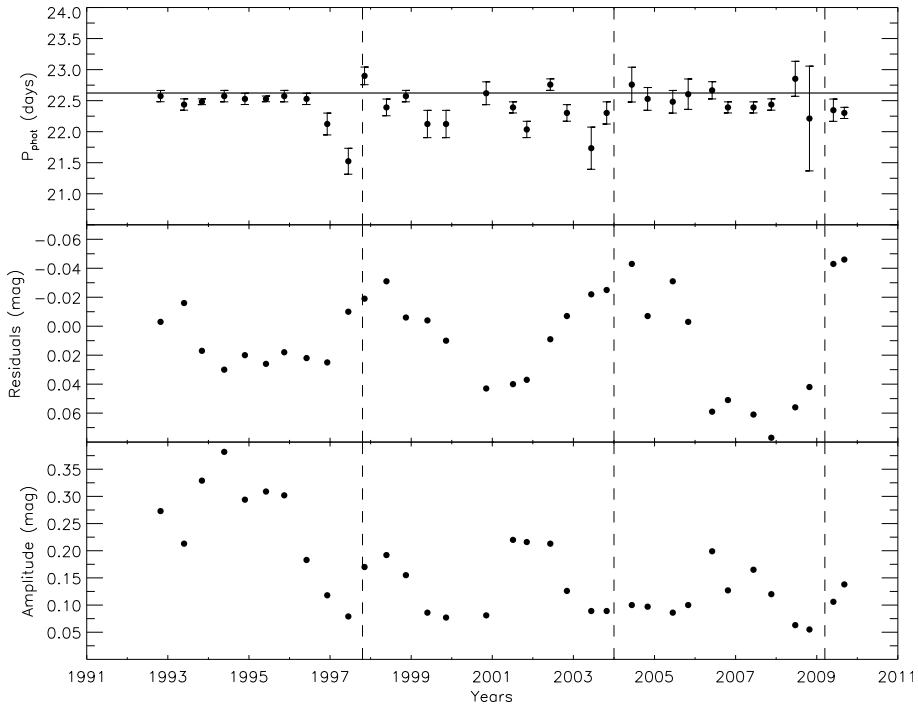

Fig. 5 Photometric period, mean brightness and amplitude variations (*from top to bottom*) of HD 208472 as a function of time. The horizontal line in the upper panel indicates the orbital period. Note that the middle panel shows the same residual as in Fig. 4 while the lower panel plots the peak-to-peak light curve amplitudes. No photometric period could be found for set #16 (year 2000.40) because the amplitude is very low and not well determined at that time.

FT is usually used to determine photometric periods but in case of active stars it is problematic because most spotted stars show asymmetrically-shaped light curves. For asymmetrical light curves, it is more efficient to use statistical methods, like Phase Dispersion Minimization (PDM; Stellingwerf 1978) or Analysis of Variances (ANOVA; Schwarzenberg-Czerny 1996). For HD 208472, we adopt the ANOVA method to determine the photometric period for all 35 subsets. The method uses periodic orthogonal polynomials to fit the light curves and then applies the variance

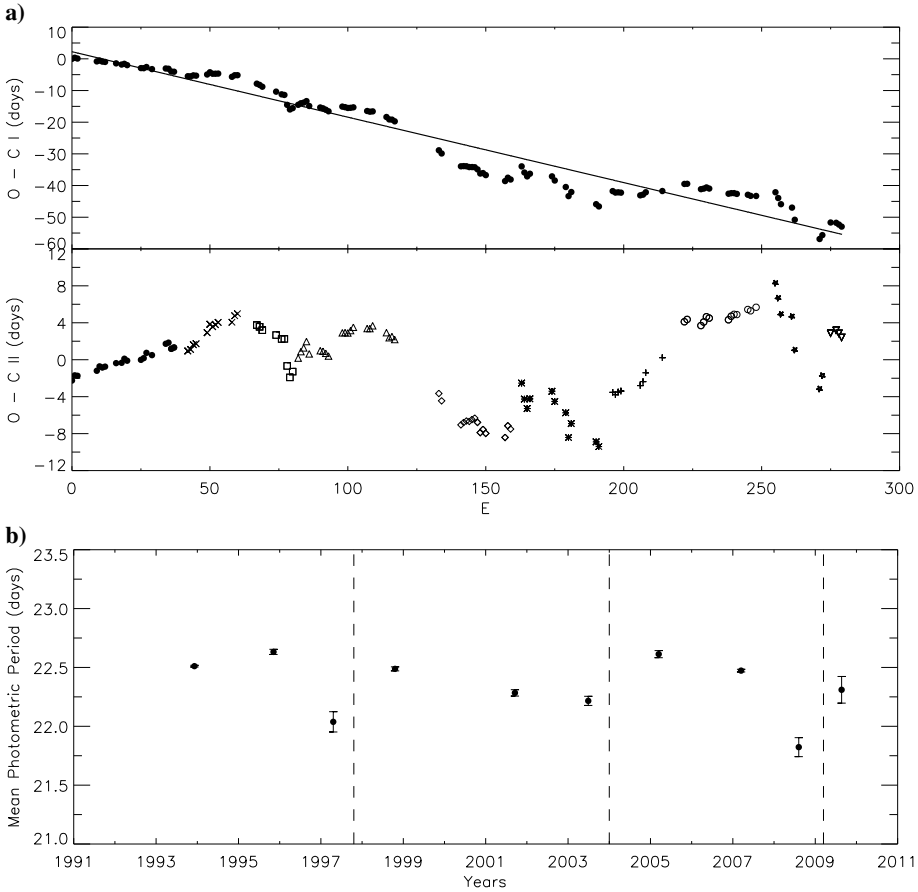

Fig. 6 *a*) $O-C$ diagram of the light-curve minima with respect to the orbital period. The straight line is a linear fit to the data according to Eq. (2). The lower panel shows the residuals. The different symbols indicate the 10 data sets that appear to fall on a nearly linear slope. *b*) The mean photometric periods from the 10 data subsets marked in the panel above.

statistics to improve the quality of the fit. We use the PERANSO software (Vanmunster 2007) to apply the method. Before the actual period analysis, we first remove the brightening trend by approximating it with a 21.5-year sinusoidal period. We believe that this brightening trend stems from a symmetric activity component which we can not resolve on the stellar surface with photometric data, e.g., like a band of spots around the star, or a polar cap-like spot (see Sect. 4.3). The resulting seasonal periods, residuals and amplitudes from the pre-whitened data are shown in Fig. 5 along with their respective errors. The numerical values are listed in Table 5. A large number of the periods seem to fall below the orbital period of the system. In case we assume a solar-like differential rotation pattern, the co-rotation latitude would be located at mid-to-high latitudes.

Figure 5 also shows that there are times of jumps of the photometric period and that they may be related to times of maximum mean brightness as well as minimum amplitude. This is indicated by the vertical dashed lines in Fig. 5. The period jumps are possibly systematic and can be brought in agreement with the 6.28-yr period of the mean brightness, which we interpreted to be due to a starspot cycle. Of course, one has to keep in mind that the period errors will increase when the amplitudes decrease, which complicates the interpretation. The early data between 1992–1996 showed the highest amplitudes and thus the most well-defined periods. While the amplitude dramatically decreased until 1997, the mean brightness started to increase from 1994 on. Therefore, the six-year period still seems a reasonable and solid estimate.

We see these period variations also from an $O-C$ analysis of light-curve minima with respect to the orbital period. The latter is assumed to be constant during the epoch of our photometric observations. We take the time of the first light-curve minimum in 1992 as the reference epoch and assume the orbital period to be the stellar rotation period. This reference epoch and the orbital period from Fekel et al. (1999) give the following ephemeris (Eq. 1):

$$T_0(\mathrm{HJD}) = 2\,448\,890.9394 + 22\overset{\mathrm{d}}{.}62293 \times E. \qquad (1)$$

The resulting $O-C$ diagram is shown in the upper panel of Fig. 6a. A linear regression fit results in the averaged ephemeris of Eq. (2):

$$T_0(\mathrm{HJD}) = \underset{(\pm 0.533)}{2\,448\,893.468} + \underset{(\pm 0.0035)}{22\overset{\mathrm{d}}{.}4149} \times E. \qquad (2)$$

The resulting period indicates that most of the spots had periods averaged around 22.4149±0.0035 days. This value is in principle agreement with the 22.54±0.05-day period

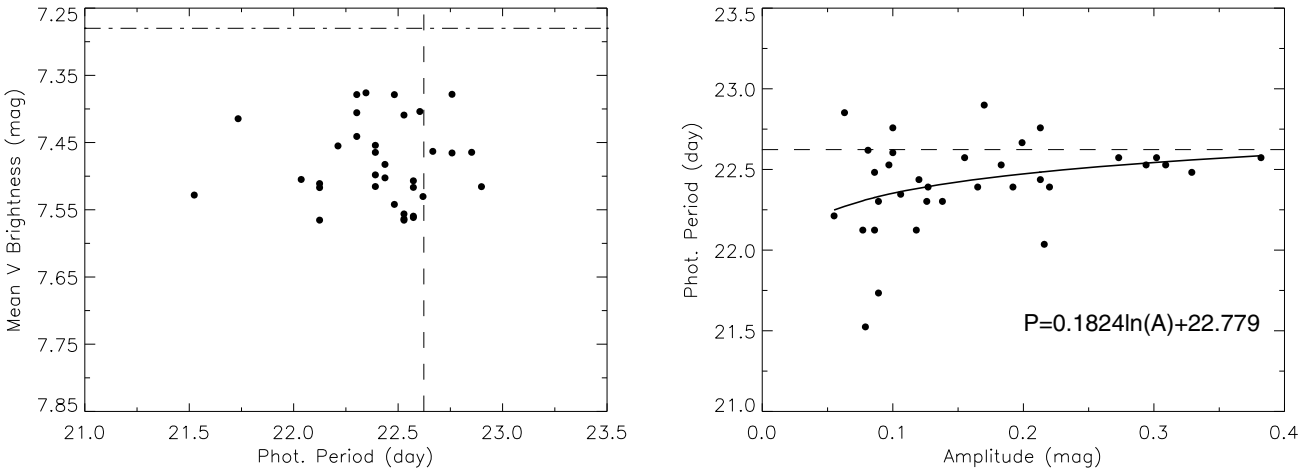

Fig. 7 *Left panel*: photometric period versus the mean brightness. There appears to be no particular correlation between the mean brightness and the photometric period other than that most photometric periods are shorter than the orbital period. The dashed-dotted line indicates the unspotted brightness level. *Right panel*: the peak-to-peak amplitude versus the photometric period. Dashed lines in both plots indicate the orbital period. The continuous line in the right panel is a logarithmic fit to the distribution as indicated in the insert (A =amplitude, P =photometric period). It indicates the trend that the amplitude from the rotational modulation becomes smaller when the photometric period is shorter.

that has been given by Henry et al. (1995) from their period analysis of an early TSU subset of the present data in that it is also shorter than the orbital period. It supports the picture that spots were preferentially located at latitudes either below or above the co-rotation latitude, only depending on whether the surface of HD 208472 rotates according to a solar-like differential rotation law or an anti-solar law in the sense that the polar regions would then rotate faster than the equatorial regions.

After removing the linear fit according to Eq. (2), we show the new residuals, dubbed $O-C$ II, in the lower panel of Fig. 6a. These residual slopes allow a determination of mean photometric periods for a given time range. For that purposes, we divide the residuals into 10 subsets by extracting portions of data that appear with a linear slope. Every slope would then give the difference between its best-fit photometric period and the grand mean period determined above. The resulting 10 periods are plotted in Fig. 6b and listed in Table 6. The distribution of periods appears similar to the ANOVA result in Fig. 5 (top panel), and can be grouped again as before. We take this as confirmation that the period variations are indeed real and that the abrupt changes are also seen from the $O-C$ analysis.

Table 6 Mean photometric periods and their errors from the $O-C$ analysis in Fig. 6b.

Year	Period (day)
1993.93	22.511 ± 0.007
1995.85	22.632 ± 0.021
1997.30	22.038 ± 0.086
1998.80	22.488 ± 0.016
2001.71	22.284 ± 0.027
2003.49	22.216 ± 0.038
2005.20	22.613 ± 0.030
2007.20	22.473 ± 0.011
2008.60	21.823 ± 0.080
2009.64	22.310 ± 0.113

4 Spot modelling

4.1 A period-amplitude-brightness relation?

Before we attempt to model the individual light curves, we investigate whether there are relations between the photometric period, the light curve amplitude and the mean brightness of the star, just as observed in the solar case and already indicated in Fig. 2. In case of the Sun, rotational periods of spots change gradually as the sunspot cycle progresses (see Fröhlich 2009). On the other hand, the mean brightness (or irradiance) of the Sun starts to increase from the beginning of the cycle towards the middle due to the more dominant facular contribution with respect to that from spots, and decreases after maximum sunspot activity towards the end of cycle. At times of maximum activity we would observe larger light curve amplitudes if we observed the Sun as a star, and the photometric period would have some average value between the maximum period (≈28 days) and the minimum period (≈25 days).

In Fig. 7, we show the distribution of the periods versus the mean brightness (left panel), and the light-curve peak-to-peak amplitude versus the period (right panel) for HD 208472. The mean V brightness does not show any particular relation to the photometric period other than that most of the periods are shorter than the orbital period. The photometric periods generally decrease with the peak-to-peak amplitude, which may indicate the end (or start) of a particular spot cycle (or lifetime cycle) on HD 208472. However, any amplitude variation might be also a conse-

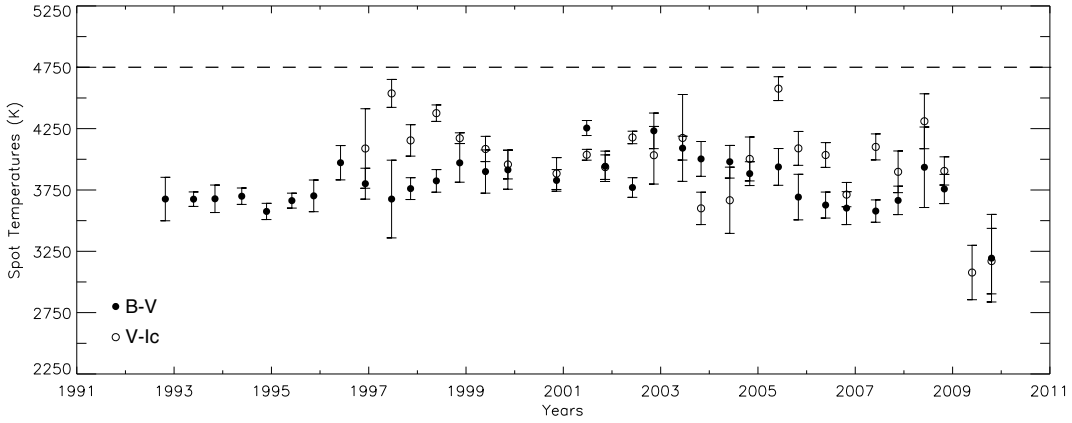

Fig. 8 Spot temperatures from $B-V$ (filled circles) and $V-I_{\rm C}$ (open circles). The horizontal dashed line indicates the unspotted photospheric temperature that we assume equal to the effective temperature of the star. Note that no $I_{\rm C}$ observations were available before 1996. For 2009.40 (data set #34), no B observations were available.

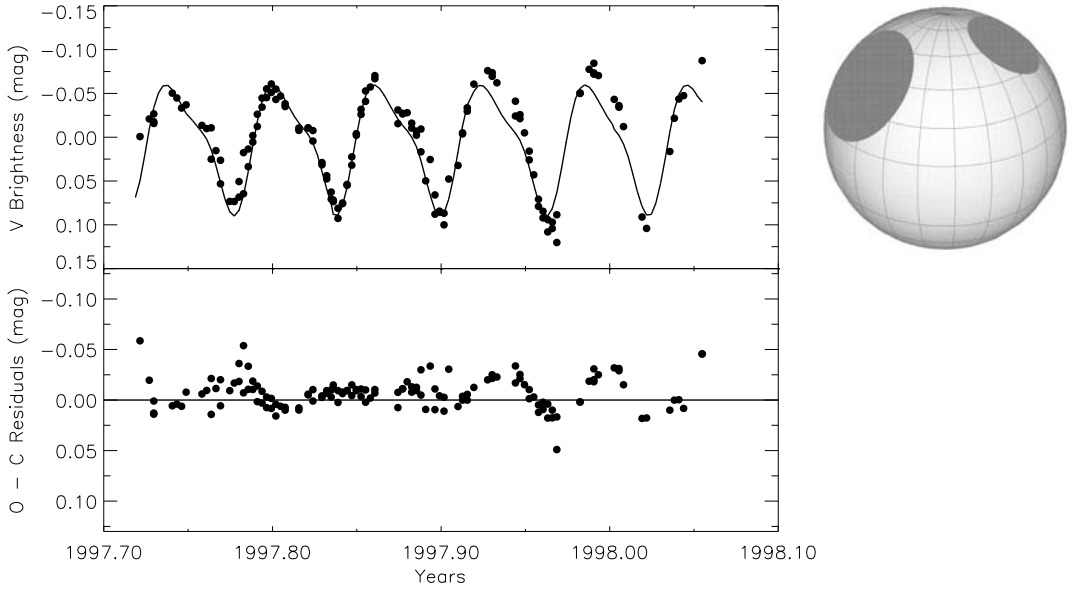

Fig. 9 An example V data set modeled with two spots (*upper panel*) and its residuals from the model fit (*lower panel*). The reconstructed spot configuration is shown in the right panel in spherical projection. Note that the residuals are systematic which just means that there was spot evolution during the time coverage of this data set (data set #11, 1997.86).

quence from a simple spot redistribution on the surface, e.g. via a break up due to the shear from differential rotation, but for HD 208472 the cyclic mean brightness variation in time supports the cycle interpretation.

4.2 Spot-model assumptions

We assume a two-spot distribution throughout the entire observing record for HD 208472. Clear asymmetries and the sometimes doubled light-curve minima per rotation are indicative of a distribution of favorably two large spots or two conglomerates of smaller spots, i.e. two active regions. It is based on the two spot model from Budding (1977) and Dorren (1987), who had negligible differences in their application though. We chose the model of Budding (1977) as implemented by Ribárik et al. (2003). In practice, we applied the code SPOTMODEL (Ribárik et al. 2003). This code allows to fit three parameters per spot (latitude, longitude, and radius) by using the Marquardt-Levenberg non-linear least squares fitting algorithm (Levenberg 1944; Marquardt 1963). The code is also able to determine spot temperatures from two color data and we employ our $B-V$ and $V-I_{\rm C}$ color curves throughout the 17 years of observation to do so. Other parameters that are assumed constant are the inclination of the rotational axis of 60° (see Sect. 3.3) and the bandpass-dependent, linear limb-darkening coefficients from van Hamme (1993).

4.3 Results

All spot modelling is done with the residual light curves after removal of the brightening trend described in Sect. 3.5. First, we calculate spot temperatures from $B-V$ and, for data taken after 1996, also from $V-I_{\rm C}$. The resulting spot

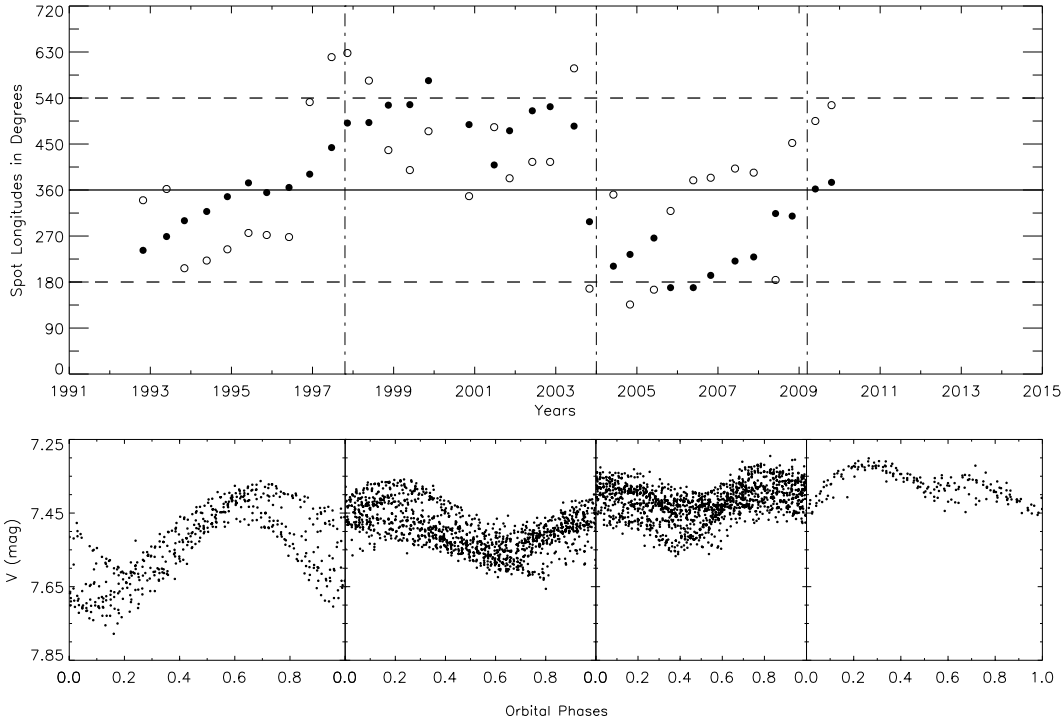

Fig. 10 The longitudinal distribution of the spots of HD 208472 (*upper panel*). The continuous line represents the longitudes of the apsidal line of the binary system while the two dashed lines just restrict one rotational cycle. The vertical dot-dashed lines correspond to times when comparably abrupt changes occurred and agree with the times already indicated in Figs. 5 and 6. The *lower panel* compares the cumulated V light curves for these intervals according to the ephemeris in Eq. (3).

temperatures for every (annual) data subset are plotted in Fig. 8. No significant cyclic or dramatic changes are seen in these spot temperatures throughout the years, except some scattering due to the sometimes very different peak-to-peak amplitudes. Intrinsic scatter comes from the different sensitivity of the B and $I_{\rm C}$ bandpasses to faculae and their time-dependent appearance, e.g., in around 1997 or around 2006. Such scatter likely causes a few hundred Kelvins of error, in particular if the B bandpass is involved. We adopt an grand average spot temperature of 3900 ± 275 K from $B-V$ and $V-I_{\rm C}$. The rms of 275 K is higher than the typical error of a seasonal spot temperature but includes intrinsic uncertainties like faculae and thus represents a fairly conservative value. Then, by assuming this spot temperature to be constant throughout the 17 years of observations, we fix the flux ratio between spot and unspotted photosphere, $k_{\rm w}$, to 0.454 and adopt it for the further modelling.

Before modelling each individual light curve, we try to constrain the expected spot latitudes. Adopting solar analogy, we implement a solar type differential rotation law on the surface of HD 208472. Because spot longitudes and radii of spots are better constraint than their latitudes, we consider the photometric periods from Table 5 (shown in Fig. 5) with respect to the co-rotation period and estimate preliminary latitudes for each of the spots and keep them fixed. We then run SPOTMODEL and calculate the remaining free parameters iteratively (longitudes and radii). After that, we take the latitudes as free parameters and, together with the longitudes and radii from the previous step, run the code again to achieve the final models. A sample light-curve fit with a representative image of the distribution of the spots is shown in Fig. 9, the actual numbers are summarized in Table 7.

We emphasize that the intrinsic spot changes due to their short-term evolution was not taken into account in our modelling. During some of the data sets, systematic variations of the light-curve shape indicated such intrinsic spot changes from one stellar rotation to the next, e.g. for the season shown in Fig. 9. Therefore, just an average "map" is obtained for each data subsets. The code always gives the model that has the statistically minimum error but sometimes these maps may not be the best representation of the spot distribution due to its inherent model limitations (circular spots). Solutions with symmetric polar caps also do not seem appropriate since previous Doppler images indicated just high and low latitude spots but no polar caps (Weber 2004) and rotationally-modulated photometry is not sensitive to such spots. For the years when the light curves appeared close to sinusoidal, like in 1994, 1995, 1996, and 2001, we repeated the calculations with iteratively altered latitudes. We were able to model 34 out of the 35 subsets. Data set #16 (year 2000.40) has very small amplitudes and no significant fit was achieved for that set. The final numerical modelling results are given in Table 7.

The spot longitudes are given with respect to the orbital ephemeris from Fekel et al. (1999) but with their epoch sub-

Table 7 Numerical results from the two-spot modelling of the 34 individual data sets. θ is the spot latitude ranging between $-90^\circ$and $+90^\circ$ (zero denotes the equator), φ is the longitude of the spot in degrees and r is the spot radius in degrees on the stellar surface.

	Spot A			Spot B		
Year	θ ($^\circ$)	φ ($^\circ$)	r ($^\circ$)	θ ($^\circ$)	φ ($^\circ$)	r ($^\circ$)
1992.82	42	242	33	48	340	23
1993.40	43	269	33	30	2	12
1993.84	47	300	40	18	207	18
1994.39	38	318	42	19	222	22
1994.90	28	347	34	35	244	28
1995.42	47	14	36	41	276	26
1995.87	49	355	38	38	272	20
1996.42	44	5	27	59	268	21
1996.93	55	31	25	51	172	9
1997.47	42	83	18	22	260	12
1997.86	42	131	28	60	268	22
1998.39	41	132	25	4	214	20
1998.87	59	166	28	50	78	17
1999.40	63	167	23	7	39	8
1999.86	14	214	16	46	115	10
2000.40	...	...	...	...	...	...
2000.86	64	128	22	2	348	21
2001.48	45	49	26	39	123	22
2001.86	63	116	35	52	23	9
2002.42	26	155	29	43	55	20
2002.86	44	163	23	43	55	20
2003.45	51	125	21	20	238	15
2003.83	53	298	22	45	167	20
2004.42	47	211	23	37	351	19
2004.83	54	234	21	56	136	16
2005.42	58	266	21	21	165	16
2005.83	33	169	20	46	319	17
2006.39	41	169	31	31	19	11
2006.82	17	193	24	1	24	13
2007.42	35	221	28	3	42	11
2007.88	46	229	24	48	34	9
2008.42	60	314	19	55	184	17
2008.83	53	309	16	52	92	9
2009.40	38	2	24	35	135	23
2009.80	11	15	25	59	166	20

tracted by one fourth of the orbital period (the star has zero eccentricity),

$$T_0(\mathrm{HJD}) = 2\,449\,246.7353 + 22\overset{\mathrm{d}}{.}62293 \times E\,. \quad (3)$$

Fekel et al.'s epoch is a time of maximum radial velocity and at that time the projection of the apsidal line of the system is perpendicular to our line of sight. Our aim is to compare the spot locations more easier, e.g., if the orbital phase in Eq. (3) is 0.0 or 0.5, then the spots are located at the substellar point or 180° opposite, respectively.

Figure 10, upper panel, shows the resulting longitudes of both spots versus time. We adopt the projected apsidal line of the system as the reference longitude and choose counter-clockwise direction for increasing longitudes. We added 360° to the longitudes of those spots that have longitudes close to a 0° or 360°, for better viewing purpose. The most striking result is that the distribution of the spot longitudes is not random but spots tend to always occur on hemispheres facing the observer during orbital quadrature. Moreover, it seems that about every six years the spots move their preferential location to the respective other hemisphere which nicely fits to our 6.2-year spot-cycle estimate from the mean brightness. Another evidence for this is shown in Fig. 10, lower panel. By following the phased light curves of consecutive years, these changes of the spot longitudes appear systematic. We interpret this with the well-known "flip-flop" phenomenon (e.g. Korhonen & Järvinen 2007; Elstner & Korhonen 2005; Järvinen et al. 2005). Furthermore, the times when the spots changed their preferential hemisphere correspond to times when the light curve amplitudes were smallest and when abrupt changes of the photometric periods were observed. During these times the star is also close to its relative maximum brightness, suggesting a vanishing overall spottedness at each end of the previous cycle and the start of a new one. Therefore, we interpret this as evidences to support our cycle estimation of 6.2 years. Accordingly, a new cycle should have just begun around 2009/2010.

4.4 Differential surface rotation

We use the photometric periods and latitudes of the corresponding data subsets to estimate the differential surface rotation of HD 208472. By assuming a solar-type, sine-squared law of the form in Eq. (4),

$$P_\theta = \frac{P_{\mathrm{equ}}}{(1 - \alpha \sin^2 \theta)}\,, \quad (4)$$

the differential-rotation coefficient $\alpha \equiv \Delta P/P = (P_\theta - P_{\mathrm{equ}})/P_{\mathrm{equ}}$ and P_{equ} is obtained iteratively from each spot (θ denotes the spot latitude and P_{equ} the equatorial rotation period). Application of a simple linear least-squares method leads to values of α = –0.003±0.011 and P_{equ} = 22.455±0.134 for spot A, and +0.011±0.009 and 22.336±0.094 for spot B. By taking the average from both spots, our best-guess values are P_{equ} = 22.395±0.114 days and α = 0.004±0.010. This α is basically a nondetection of differential rotation and disagrees with the value from the sheared-image Doppler reconstruction by Weber (2004) of -0.04. Note though that photometry can not determine the true sign of the differential-rotation parameter and is implicitly assumed positive here. However, its amount – if positive or negative – suggests differential rotation significantly weaker compared to the Sun.

5 Summary and conclusions

Chromospherically active stars have light variations caused by spots rotating in and out of view, enabling the rotation period of the star to be determined for the surface latitude of the spot. However, such latitude dependent rotation will smear out the observed rotational period if one

has only short chunks of photometry and it takes long time coverage and good sampling to resolve these periods. By analyzing our 17 years of time-series photometric data of HD 208472, we explored the relation between photometric periods, light-curve amplitudes, mean brightness and the color of the star, spot latitudes and longitudes and arrived at following results.

Firstly, we found evidence for a 6.28±0.06-yr brightness cycle, which we interpret to be a stellar analog of the solar 11-year sunspot cycle. There is also evidence for a second, longer cycle, approximated with a 21.5±0.5-yr period, which could be interpreted as the stellar analog of the solar Gleissberg cycle (Kolláth & Oláh 2009). While the long-term mean brightness increases, all color indices tend to get bluer and the rotationally modulated light-curve amplitudes smaller. So far, the star had its maximum brightness level in 2010 and likely was then very close to being unspotted, in agreement with the expectations from a cool spot model. On the other hand, the latest data indicate that the brightness of the star is still rising.

Secondly, we found that the distribution of the spot longitudes is not random but spots tend to always occur on hemispheres facing the observer during orbital quadrature. It appeared that about every six years the spots moved their preferential location to the respective other hemisphere, in agreement with the 6.2-year spot cycle obtained from the mean brightness. We interpret this as evidence for a "flip-flop" dynamo behavior (Elstner & Korhonen 2005) because when the spots changed their preferential hemisphere the light curve amplitudes were always the smallest and abrupt changes of the photometric periods occurred. During such flips, or flops, the star was always close to its relative maximum brightness, suggesting that we witnessed a spot minimum. However, the 17 years of data allowed the monitoring of just two such "flips" and at least one "flop", and therefore can not be taken fully conclusive at that point. Because a flip was possibly observed in 2009/10, we predict an according flop near 2015/16.

Thirdly, our two-spot modelling is consistent with a differential-rotation coefficient of $\alpha = \Delta P/P$ of 0.004 ± 0.010, almost fifty times weaker than for the Sun, but basically represents a non detection of differential rotation.

Acknowledgements. OÖ greatly acknowledges supports from the Turkish Scientific and Technical Research Council TÜBİTAK and Ege University Science Fund, under Project No. 2008/Fen/061. OÖ is also grateful to the Stellar Activity Group at AIP for their friendly and warm hospitality during his PhD works at AIP. OÖ also thanks to G. Taş et al. for allowance to use their 1996 and 1997 data, which they published in the scope of the project "Ege University Science Fund, Project No. 96/Fen/026". KGS appreciates the continuous support of the operation of the APTs in southern Arizona from the State of Brandenburg. We are all thankful to Louis Boyd at Fairborn Observatory without whose detailed efforts our APTs would have not been so effective. This study has made use of the SIMBAD database, operated at CDS, Strasbourg, France.

References

Amado, P.J.: 2003, A&A 404, 631
Andruk, V., Kharchenko, N., Schilbach, E., Scholz, D.: 1995, AN 316, 225
Berdyugina, S.V.: 2005, Living Rev. Solar Physics 2, 8
Budding, E.: 1977, Ap&SS 48, 207
Dorren, J.D.: 1987, ApJ 320, 756
Drilling, J.S., Landolt, A.U.: 2000, in: A.N. Cox (ed.), *Allens Astrophysical Quantities*, 4th ed., p. 381
Elstner, D., Korhonen, H.: 2005, AN 326, 278
Erdem, A., Budding, E., Soydugan, E., Bakis,, H., Dogru, D., Dogru, S.S., Tüysüz, M., Kacar, Y., Dönmez, A., Soydugan, F.: 2009, New A 14, 545
Fekel, F. C., Henry, G. W., Eaton, J. A., Sperauskas, J., Hall, D. S.: 2002, AJ 124, 1064
Fekel, F.C., Strassmeier, K.G., Weber, M., Washuettl, A.: 1999, A&AS 137, 369
Fitzpatrick, E.L.: 1999, PASP 111, 63
Flower, P.J.: 1996, ApJ 469, 355
Fröhlich, C.: 2009, A&A 501, L27
Genet, R.M., Boyd, L.J., Baliunas, S.L.: 1986, International Amateur-Professional Photoelectric Photometry Communication25, 15
Granzer, T., Reegen, P., Strassmeier, K.G.: 2001, AN 322, 325
Gray, D.F.: 2005, *The Observation and Analysis of Stellar Photospheres*, 3rd ed., Cambridge Univ. Press
Hall, D.S.: 1972, PASP 84, 323
Hardie, R.H.: 1962, in: W.A. Hiltner (ed.), *Astronomical Techniques*, p. 178
Hauck, B., Mermilliod, M.: 1998, A&AS 129, 431
Henry, G.W.: 1995a, in: G.W. Henry, J.A. Eaton (eds.), *Robotic Telescopes. Current Capabilities, Present Developments, and Future Prospects for Automated Astronomy*, ASPC 79, p. 37
Henry, G.W.: 1995b, in: G.W. Henry, J.A. Eaton (eds.), *Robotic Telescopes. Current Capabilities, Present Developments, and Future Prospects for Automated Astronomy*, ASPC 79, p. 44
Henry, G.W., Fekel, F.C., Hall, D.S.: 1995, AJ 110, 2926
Hilker, M.: 2000, A&A 355, 994
Järvinen, S., Berdyugina, S., Strassmeier, K.G.: 2005, A&A 440, 735
Koen, C., Eyer, L.: 2002, MNRAS 331, 45
Kolláth, Z., Oláh, K.: 2009, A&A 501, 695
Korhonen, H., Järvinen, S.P.: 2007, in: W.I. Hartkopf, E.F. Guinan, P. Harmanec (eds.), *Binary Stars as Critical Tools & Tests in Contemporary Astrophysics*,IAU Symp. 240, p. 453
Lenz, P., Breger, M.: 2005, Communications in Asteroseismology 146, 53
Levenberg, K.: 1944, Quart. Appl. Math. 2, 164
Marquardt, D.W.: 1963, SIAM J. Appl. Math. 11, 431
Oláh, K., Kövari, Zs., Bartus, J., Strassmeier, K.G., Hall, D.S., Henry, G.W.: 1997, A&A 321, 811
Ribárik, G., Oláh, K., Strassmeier, K.G.: 2003, AN 324, 202
Schwarzenberg-Czerny, A.: 1996, ApJ 460, L107
Stellingwerf, R.F.: 1978, ApJ 224, 953
Strassmeier, K.G.: 2009, A&A Rev. 17, 251
Strassmeier, K.G., Bopp, B.W.: 1992, A&A 259, 183
Strassmeier, K.G., Hall, D.S., Henry, G.W.: 1994, A&A 282, 535
Strassmeier, K.G., Boyd, L.J., Epand, D.H., Granzer, T.: 1997, PASP 109, 697
Strassmeier, K.G., Serkowitsch, E., Granzer, T.: 1999, A&AS 140, 29
van Hamme, W.: 1993, AJ 106, 2096

van Leeuwen, F.: 2007, A&A 474, 653
Vanmunster, A.: 2007, http://www.peranso.com/
Weber, M.: 2004, PhD Thesis, University of Potsdam
Weber, M., Strassmeier, K.G., Washuettl, A.: 2001, in: R.E. Schielicke (ed.), JENAM 2001, Astron. Ges. Abstract Series Vol. 18, P 89
Weber, M., Strassmeier, K.G., Washuettl, A.: 2005, AN 326, 287

A Transformation coefficients for the EUO photometric data

Equations (A1) and (A2) are for the EUO Johnson and Strömgren measurements, respectively:

$$
\begin{aligned}
&V - v_0 = -0.050(\pm0.017) \times (B-V) + 18.674(\pm0.013),\\
&B - V = 1.115(\pm0.015) \times (b-v)_0 + 0.608(\pm0.008),\\
&U - B = 1.063(\pm0.031) \times (u-b)_0 - 1.849(\pm0.064),\\
&V - R = 1.174(\pm0.026) \times (v-r)_0 + 1.272(\pm0.021); \qquad \text{(A1)}
\end{aligned}
$$

$$
\begin{aligned}
&V - y = 0.046(\pm0.019) \times (b-y) + 17.220(\pm0.007),\\
&b - y = 1.028(\pm0.010) \times (b-y)_0 + 0.173(\pm0.03),\\
&m_1 = -0.175(\pm0.037) + 1.099(\pm0.137) \times (m_1)_0 +\\
&\qquad + 0.031(\pm0.056) \times (b-y),\\
&c_1 = 0.229(\pm0.035) + 1.042(\pm0.066) \times (c_1)_0 -\\
&\qquad - 0.049(\pm0.053) \times (b-y),\\
&\mathrm{H}_\beta = 1.110(\pm0.199) \times (\mathrm{H}_\beta)_0 + 0.581(\pm0.378). \qquad \text{(A2)}
\end{aligned}
$$

